Th B4 09

Estimating Structural Uncertainties in Seismic Images Using Equi-probable Tomographic Model

J. Messud* (CGG), P. Guillaume (CGG), G. Lambaré (CGG)

Summary

Assessing the uncertainty of the structural information contained in seismic images is critical for reservoir risk analysis, namely reservoir delineation, reserve estimation, and well planning. We propose here a distinctive approach aimed at assessing structural uncertainties associated with ray-based tomography. While it has some similarities with previously published approaches, it is based on the random generation of equi-probable tomographic models rather than on randomly sampling the a posteriori "probability density function". Moreover it is associated with non-linear slope tomography which allows consideration of some non-linear aspects of the problem. We believe these two aspects offers significant advantages in terms of efficiency and accuracy. In this paper we carefully review the concepts and definitions (in particular the notions of confidence region and error bars), and then present our approach and discuss its advantages. We finally present an application to a North Sea dataset where we estimate structural error bars for a target horizon.

Introduction

Seismic imaging aims at positioning reflectors in the subsurface from a set of observed reflection data. Resulting images are used in combination with other information (e.g. well data) for building stratigraphic models of reservoirs. These models allow for reservoir delineation, well planning, and evaluation of reserves and production risks. For this the uncertainties from each source of information must be considered. Those associated with seismic imaging, especially in the context of velocity model building ("velocity" here being meant in the broad sense, i.e. it includes the anisotropy parameters) are crucial for positioning migrated structures and have only been investigated recently. For example, Duffet and Sinoquet (2006) and Osypov et al. (2008, 2013) investigated the structural uncertainties associated with ray-based tomography, the most widely used tool for migration velocity model building. These works involve two steps: generation of a set of tomographically consistent models, then computation of statistics on structural properties of the images. Several industrial applications have been published arousing considerable interest (Osypov et al., 2013).

Here we propose a new strategy aiming at assessing structural uncertainties associated with ray-based tomography. While the goal and the general steps are the same as in Osypov et al. (2013) we have developed a distinctive approach: generation of equi-probable tomographic models rather than sampling of a "probability density function". By being associated with non-linear slope tomography (Guillaume et al., 2013) the method considers some non-linear aspects of the problem. We first present the theoretical frame of our approach, emphasizing the concepts (in particular the notions of confidence region and error bars) and its advantages, before presenting an application.

Tomography probability density function

Non-linear slope tomography is an essential tool for velocity model building (Guillaume et al., 2013). Its input data consists of a set of "invariants" (i.e. source and receiver positions, and time and slopes of locally coherent events in the un-migrated domain). The tomography model is described by a set of parameters describing smooth velocity and anisotropy layers separated by horizons. The model is updated through a non-linear optimization scheme aiming at minimizing the residual move-out.

Let us consider a final tomography model described here by a vector $\boldsymbol{m}_0$ of dimension N. In practice N ranges from 500,000 to 50 million. Despite the quality of the resolution of the tomographic inversion problem, by its very nature $\boldsymbol{m}_0$ is uncertain as the tomography input data, modeling, and constraints contain uncertainties. Bayesian theory considers the related uncertainties in $\boldsymbol{m}_0$ using the concept of probability density functions (PDF). Within the Gaussian and linearized approximation of the tomographic forward operator, the PDF, $\widetilde{\rho_M}(\Delta\boldsymbol{m})$, of a perturbation $\Delta\boldsymbol{m}$ around $\boldsymbol{m}_0$ takes a Gaussian distribution (Tarantola, 2005)

$$\widetilde{\rho_M}(\Delta\boldsymbol{m}) \propto exp\left\{-\frac{1}{2}\Delta\boldsymbol{m}^+ \widetilde{\boldsymbol{C}_M}^{-1} \Delta\boldsymbol{m}\right\} \quad , \qquad \widetilde{\boldsymbol{C}_M}^{-1} = \boldsymbol{G}_0^+ \boldsymbol{C}_D^{-1} \boldsymbol{G}_0 \; + \boldsymbol{C}_M^{-1} \qquad . \qquad (1)$$

The $N \times N$ matrix $\widetilde{\boldsymbol{C}_M}^{-1}$ is called the tomography Hessian. Its inverse is the a posteriori covariance matrix $\widetilde{\boldsymbol{C}_M}$ defined by the combination of the linearized tomographic forward operator in $\boldsymbol{m}_0$, $\boldsymbol{G}_0$, the data covariance matrix containing quality factors, $\boldsymbol{C}_D$, and the a priori covariance matrix containing model constraints, $\boldsymbol{C}_M$. It (or more specifically $\boldsymbol{C}_M^{-1}$) includes, amongst other contributions, a Tikhonov regularization expressed as $\varepsilon \boldsymbol{I}_N$ in a basis where all model components have the same units, ε being the "damping" level. "$^+$" denotes the matrix transpose.

$\boldsymbol{m}_0$ does not necessarily represent the true subsurface velocity or the optimum migration model. It represents the maximum-likelihood model, i.e. the most probable model according to the set of data and constraints. But many other probabilistically pertinent models exist. $\widetilde{\rho_M}(\Delta\boldsymbol{m})$ allows a characterization of these models as it provides the probabilities associated with perturbations $\Delta\boldsymbol{m}$.

Definitions

It is crucial within reservoir risk analysis to give a precise definition of what we mean by uncertainty. Uncertainties can be associated with a probability P (or confidence level) and defined as a region of the model space such that there is a probability of P that the true model belongs to the region (Cowan, 1998). One might think to characterize uncertainties through an error bar vector $\boldsymbol{a}$ constructed so as to have a given confidence level P that the true model is contained within the domain $\boldsymbol{m}_0 \pm \boldsymbol{a}$. This

turns out to be computationally difficult, and is rarely done in the general case to paraphrase Cowan (1998, §2.7). Nevertheless uncertainties are sometimes defined through an error bar vector $\boldsymbol{\sigma}$ containing the square roots of the diagonal elements of $\widetilde{\boldsymbol{C}_M}$, called a posteriori standard deviations (Duffet and Sinoquet, 2006; Tarantola, 2005). This has a meaning only if the correlations (or non-diagonal elements of $\widetilde{\boldsymbol{C}_M}$) are negligible, and even then not straightforwardly in terms of a confidence level. This is not suited for tomography where correlations may be large (Duffet and Sinoquet, 2006).

To overcome these limitations we must define uncertainties through the tomography confidence region related to a probability *P* (Cowan, 1998). Let us consider the region of the model space for which the PDF values are greater than a given value, i.e. $\widetilde{\rho_M}(\Delta\boldsymbol{m}) \geq constant$. Integrating $\widetilde{\rho_M}$ inside this region gives the probability that the region contains the true value of $\Delta\boldsymbol{m}$:

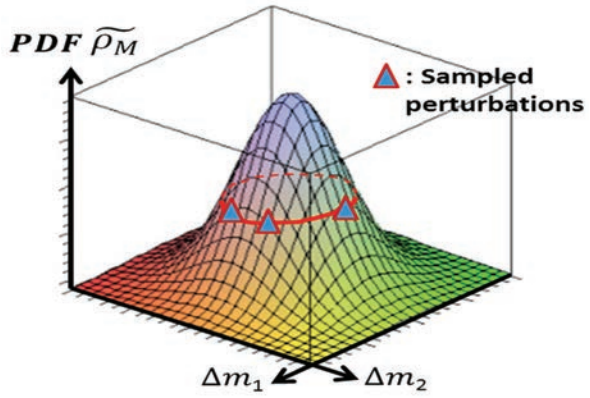

Figure 1 *PDF of a perturbation* $\Delta\boldsymbol{m}$ *(N=2) and equi-probable "hyper-ellipsoidal" contour (red).*

$$"Probability\ that\ \Delta\boldsymbol{m_{true}} \in region" = P \quad (2)$$

Conversely consider a "centered" region related to a confidence level *P*. The boundary of the region is defined by a equi-probable hyper-ellipsoidal contour of the PDF ($\widetilde{\rho_M}(\Delta\boldsymbol{m}) = constant$) through

$$\Delta\boldsymbol{m}^+ \widetilde{\boldsymbol{C}_M}^{-1} \Delta\boldsymbol{m} = Q_N(P) \quad (3)$$

where $Q_N(P)$ is the quantile of order *P* of the Chi-square distribution of the *N*-dimensional problem (Cowan, 1998). Resolving equation (3) gives the boundary (or "maximum possible") equi-probable perturbations of the *P* confidence region, see Figure 1 for an illustration.

In the following we use *P=68.3%* for the confidence region. We call it the standard deviation-like confidence region (Messud et al., 2017) because it leads to a standard deviation interval when *N=1* or when model parameters are non-correlated and considered independently (Duffet and Sinoquet, 2006).

Generating equi-probable models

It is easy to show that the solutions to equation (3) will be given by

$$\Delta\boldsymbol{m} = \sqrt{Q_N(P)}\boldsymbol{B}\,\boldsymbol{\delta r} \quad , \quad \boldsymbol{\delta r}^+\boldsymbol{\delta r} = 1 \quad , \quad \boldsymbol{B}\boldsymbol{B}^+ = \widetilde{\boldsymbol{C}_M} \quad (4)$$

where $\boldsymbol{\delta r}$ is a unit random vector allowing to generate the solutions and $\boldsymbol{B}$ is a "square root" of $\widetilde{\boldsymbol{C}_M}$. We approximate $\boldsymbol{B}$ through an eigenvalue decomposition (EVD) of the Hessian (Zhang and McMechan, 1995) stopped when the eigenvalues have reached the fixed a priori damping level ε. Thus

$$\boldsymbol{D}^+\widetilde{\boldsymbol{C}_M}^{-1}\boldsymbol{D} \approx \boldsymbol{V}_p\,\Delta_p\boldsymbol{V}_p^+ + \varepsilon\boldsymbol{I}_N \quad (5)$$

where *p* is the number of eigenvectors above ε. $\boldsymbol{V}_p$ and Δ_p contain the *p* eigenvectors and eigenvalues, respectively. Because the EVD cannot mix different physical quantities we introduced the diagonal and invertible matrix $\boldsymbol{D}$ that simply rescales the various physical units in the model space and may somewhat compensate for subsurface illumination. Interestingly, $\varepsilon\boldsymbol{I}_N$ approximates the effect of the non-computed $N-p$ eigenvectors $\boldsymbol{V}_{N-p}$ assuming $\boldsymbol{V}_{N-p}\boldsymbol{V}_{N-p}^+ \underset{N\gg p}{\longrightarrow} \boldsymbol{I}_N$. After manipulations we obtain

$$\boldsymbol{B} = \boldsymbol{B}^{resolved} + \boldsymbol{B}^{un-resolved} \quad (6)$$

$$\boldsymbol{B}^{resolved} = \boldsymbol{D}\boldsymbol{V}_p\left(\Delta_p + \varepsilon\boldsymbol{I}_p\right)^{-1/2}\boldsymbol{V}_p^+ \quad , \quad \boldsymbol{B}^{un-resolved} = \boldsymbol{D}(\boldsymbol{I}_N - \boldsymbol{V}_p\boldsymbol{V}_p^+)\varepsilon^{-1/2}$$

The method allows to separate the contribution of the uncertainties in the tomographically "resolved subspace" (namely the $\boldsymbol{B}^{resolved}$ term related to the model subspace spanned by eigenvectors above the a priori damping level) from the total uncertainties ($\boldsymbol{B}$). Equations (4) and (6) allow finding solutions of equation (3) by considering various random vectors $\boldsymbol{\delta r}$ (of dimension *N)*.

Error bars for horizons

In Guillaume et al. (2013) while velocity parameters of the layers are updated tomographically at each iteration, horizons are updated by map (or zero-offset kinematic) migration of "horizon invariants".

The maximum likelihood horizon, obtained by map migration in $\boldsymbol{m}_0$, is described by a vector $\boldsymbol{h}_0$ whose parameters are the depth of the horizon for any surface position. Once the model perturbations are obtained, i.e. a set of solutions $\{\Delta\boldsymbol{m}\}$ of equation (3), we can perform map migrations of the horizon for each $\Delta\boldsymbol{m}$ to obtain a set of horizon perturbations $\{\Delta\boldsymbol{h}\}$ around $\boldsymbol{h}_0$ for statistical analysis.

To interpret the results let us consider the "linearized approximation" of the horizon map migration operator $\boldsymbol{H}^+$: $\Delta\boldsymbol{h} \approx \boldsymbol{H}^+ \Delta\boldsymbol{m}$. The migration PDF is then defined by the a posteriori covariance matrix

$$\widetilde{\boldsymbol{C}_H} = \boldsymbol{H}^+ \widetilde{\boldsymbol{C}_M} \boldsymbol{H} \tag{7}$$

It contains information on migration uncertainties related to the tomography model used by the migration algorithm. Thus we can interpret the set $\{\Delta\boldsymbol{h}\}$ of horizon perturbations, as a set of equi-probable (and maximum possible) horizon perturbations within the *P=68.3%* confidence region.

Let us now define error bars $\Delta\theta_i$ as the maximum possible depth variations of a horizon parameter within the confidence region: $\Delta\theta_i = \max\{|\Delta h_i|\}$. $\Delta\boldsymbol{\theta}$ is a depth error bar. Obviously horizons move vertically and laterally for each migration in $\Delta\boldsymbol{m}$. $\Delta\boldsymbol{\theta}$ considers the depth "envelope" of all migrated horizons and thus also accounts for lateral displacements of migrated points. The true horizon depth position belongs to $\boldsymbol{h}_0 \pm \Delta\boldsymbol{\theta}$ with probability $P \geq 68.3\%$. As $\Delta\boldsymbol{\theta}$ is related to a *68.3%* confidence level we sometimes call it the z-direction standard deviation-like attribute (Messud et al., 2017).

Originalities of our method

Our formal results present similarities with the ones of (Osypov et al., 2013) but we see two major novelties. First we propose to sample a PDF's hyper-ellipsoid contour to obtain equi-probable velocity perturbations whereas Osypov et al. (2013) sample the full PDF and derive statistical properties from it. Secondly we use our approach within the frame of non-linear slope tomography.

The first point reduces the sampled space to its most representative "dimensions" in terms of uncertainties, thus optimizing the random exploration. Typically we obtain stable depth error bars with 200-500 random models, without introducing any preconditioning that reduces the dimensionality of the model space (for example, Osypov et al. (2013) use steering filters). Note also that restricting the sampled space like this does not hamper the assessment of the uncertainties compared to the sampling of the full PDF because the sampled hyper-ellipsoid fully characterizes the full PDF (all hyper-ellipsoids are related by a proportionality constant, see equations (3) and (4)).

Regarding the second point, the use of a non-linear approach based on kinematic invariants, i.e. non-linear slope tomography, provides an efficient way to assess the quality of the randomly generated model perturbations. For example, the cost functions related to the perturbations can be estimated automatically and non-linearly allowing the consideration of some non-linear aspects of the problem. This shows that a perturbation selection step seems unnecessary with our method as discussed below.

North Sea data example

The method is illustrated on a North Sea data example where 500 model perturbations were generated. Figure 2 shows, for the 100 first perturbations, the non-linearly computed tomography cost functions (that become equal to $\Delta\boldsymbol{m}^+ \widetilde{\boldsymbol{C}_M}^{-1} \Delta\boldsymbol{m}$ up to a constant in the linear approximation). It is obvious that almost iso-cost (i.e. equi-probable) $\Delta\boldsymbol{m}$ were generated. We observe only limited variations around the average cost function value of the perturbed models meaning that the linear hypothesis assumed in our analysis is appropriate. Moreover we see that it is not necessary to remove non-pertinent perturbations related to too large variations of the cost function.

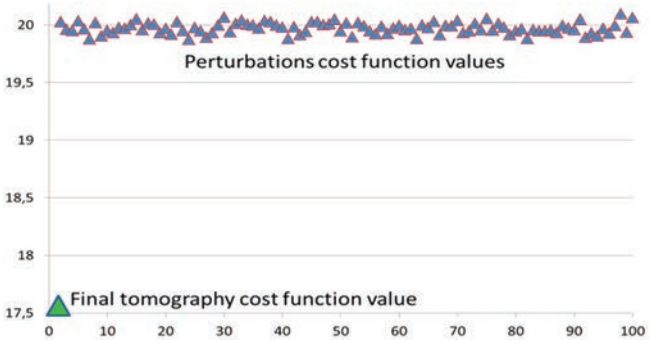

Figure 2 *Tomography cost functions related to the 100 first sampled model perturbations (North Sea data).*

Four different surveys (labelled A-D in Figure 3a) have been acquired in the area over time. Each survey was shot with a different acquisition direction (illustrated by the arrows in Figure 3a) and its own specific recording configuration.

Figure 3b shows the computed depth error bars of the top chalk. A clear correlation can be observed between the illumination map in Figure 3a and the uncertainty map in Figure 3b. Areas with overlapping surveys, i.e. multi-azimuth illumination, show lower uncertainties. Lower-fold areas such as the rig zone inside survey C result in relatively higher uncertainties correlated to the reduction in tomographic ray angular diversity. Also we observe larger uncertainties on the survey edges.

Only total uncertainties, that tend to highlight the acquisition illumination and structural complexity, are shown in Figure 3. The resolved subspace contribution gives complementary information that tends to highlight how illumination diversity drives the tomography discrimination capability (Messud et al., 2017).

Conclusion

We have presented a new strategy for computing uncertainties in tomography models, and translating them into the migrated domain. Standard deviations-like attributes on horizon depth positions are computed. Our approach is original, in particular the generation of equi-probable models, and allows considering some non-linear aspects of the problem.

Acknowledgments

We thank PremierOil, Edison, and Bayerngas for their permission to show the data. We thank CGG for their permission to publish this work. We gratefully thank Mathieu Reinier for his involvement. We thank Thibaut Allemand, Jean-Philippe Montel and Andrew Ratcliffe for insightful remarks.

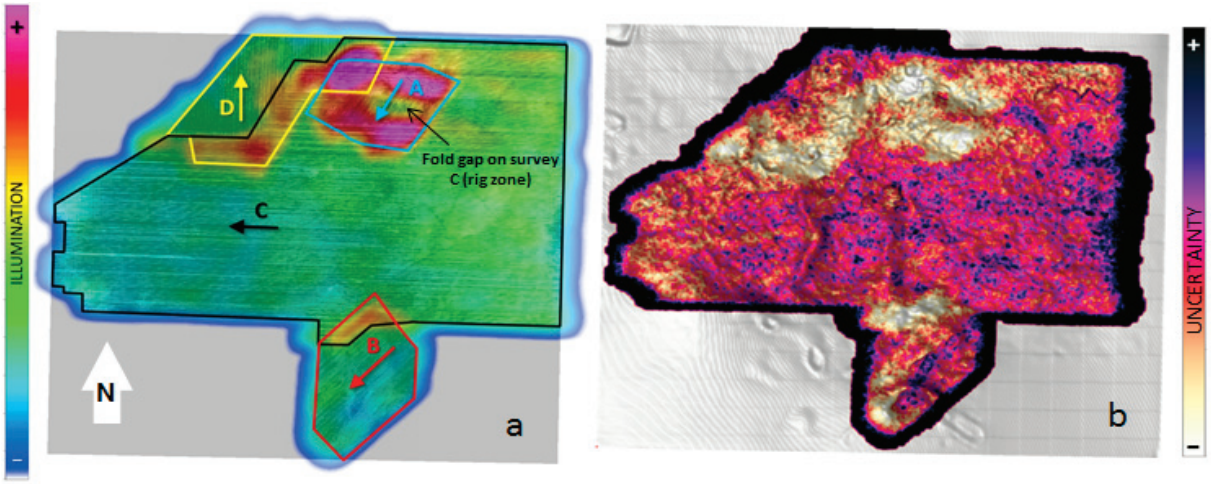

Figure 3 *North Sea data Top Chalk horizon attributes: (a) illumination map, (b) total depth error bars (z-direction standard deviation-like attribute). Figure from (Messud et al., 2017).*

References

Cowan, G. [1998] Statistical Data Analysis. *Oxford Science Publication*, Oxford.

Duffet, C. and Sinoquet, D. [2006] Quantifying uncertainties on the solution model of seismic tomography. *Inverse Problems*, **22**, 525-538.

Guillaume, P., Zhang, X., Prescott, A., Lambaré, G., Reinier, M, Montel, J-P and Cavalié, A. [2013] Multi-layer non-linear slope tomography. *75th EAGE Conference & Exhibition*, Extended Abstracts, Th 04 01.

Messud, J., Reinier, M., Prigent, H., Guillaume, P., Coléou, T. and Masclet, S. [2017] Extracting seismic uncertainties from tomographic velocity inversion and their use in reservoir risk analysis. *The Leading Edge*, in press (February).

Osypov, K., Nichols, D., Woodward, M., Zdraveva, O. and Yarman, CE [2008] Uncertainty and resolution analysis for anisotropic tomography using iterative eigendecomposition. *SEG*, Extended Abstracts, 3244.

Osypov, K., Yang, Y., Fourier, A., Ivanova, N., Bachrach, R., Yarman, C. E., You, Y., Nichols, D. and Woodward, M. [2013] Model-uncertainty quantification in seismic tomography: method and applications. *Geophysical Prospecting*, **61**, 1114-1134.

Tarantola, A. [2005] Inverse Problem Theory and Methods for Model Parameters Estimation. *Society for Industrial and Applied Mathematics*, Philadelphia.

Zhang, J. and McMechan, G. A. [1995] Estimation of resolution and covariance for large matrix inversions. *Geophysical Journal International*, **121**, 409-426.